Surface & Coatings Technology 217 (2013) 84–87

Contents lists available at SciVerse ScienceDirect

Surface & Coatings Technology

journal homepage: www.elsevier.com/locate/surfcoat

Solid solution coating of (TiVCrZrHf)N with unusual structural evolution

Du-Cheng Tsai [a], Zue-Chin Chang [b], Li-Yu Kuo [a], Tien-Jen Lin [a], Tai-Nan Lin [c], Fuh-Sheng Shieu [a,*]

[a] Department of Materials Science and Engineering, National Chung Hsing University, Taichung 40227, Taiwan
[b] Department of Mechanical Engineering, National Chin-Yi University of Technology, Taichung 41170, Taiwan
[c] Chemical Engineering Division, Institute of Nuclear Energy Research, Taoyuan County, 32546, Taiwan

ARTICLE INFO

Article history:
Received 27 August 2012
Accepted in revised form 29 November 2012
Available online 7 December 2012

Keywords:
Coating materials
Nitride materials
Microstructure

ABSTRACT

In this study, we investigated the microstructure of (TiVCrZrHf)N multi-element coating deposited on Si(100) substrate by magnetron sputtering system. Interestingly, the film showed an unusual structure evolution. A continuous and amorphous initial (TiVCrZrHf)N layer formed on the substrate. As film thickness increased, randomly oriented small (TiVCrZrHf)N grains formed, followed by the development of columnar grains with FCC crystal phase. In contrast to previous studies, the nitride coatings grew on substrates with a 270-nm amorphous interlayer. Under appropriate parameters, the occurrence of the unusual microstructure could be attributed to the sluggish diffusion of the multi-principal components. The maximum hardness of 33.5 GPa was obtained when coating was deposited under substrate bias of −100 V and at substrate temperatures of 723 K.

1. Introduction

The synthesis of novel multi-principal component nitride coatings, such as (AlCrTaTiZr)N [1], (AlCrNbSiTiV)N [2], and (AlMoNbSiTaTiVZr)N [3], has attracted extensive research interest due to their excellent physical and chemical properties, which are expected to be superior to those of binary or ternary nitride coatings. From a thermodynamics perspective, the high mixing entropies contributed by multi-principal components are believed to stabilize the existence of simple solid solution structures. A single FCC solid solution structure has been reported for multi-principal component nitrides. From a kinetics perspective, large lattice distortions caused by differently-sized atoms lower the diffusion rates of atoms and thus reduce the growth rate of crystallites [4–6]. The resulting coatings are of great interest as potential hard coatings because of their good mechanical properties due to lattice distortions and solid solution strengthening. In addition, they have also received considerable interest as diffusion barriers for Cu interconnections. Further research and development can yield coatings with various functions and great potential for application in different fields [7].

Recently, (TiVCrZrHf)N coatings with five strong nitride forming elements were designed to deposit strong nitride coatings by reactive radio-frequency (RF) magnetron reactive sputtering [8–11]. Material selection was based on the properties of individual binary nitride. Ti and Cr were selected as constituents, since TiN and CrN have been widely used as protective surface coatings due to their satisfactory mechanical properties. To further improve thermal stability, oxidation resistance, and corrosion resistance, Zr and Hf were incorporated into cubic nitride structure because of their great negative free energy of formation. The addition of V into TiN and CrN had demonstrated low friction coefficient due to the solid state lubricious properties of vanadium oxides. In previous studies, the (TiVCrZrHf)N coatings exhibited a simple FCC structure and that their five metallic elements were in a near-equimolar ratio (not shown). According to the rule of mixtures, the lattice spacing (0.253 nm) of the (TiVCrZrHf)N approximated the average of the fcc (111) planes of TiN, VN, CrN, ZrN, and HfN. This finding exhibited the formation of a simple solid solution with an fcc structure from constituent nitrides and confirmed the effect of high entropies on the simplification of crystal structures. Depth profiling analyses of elemental distributions (SIMS, ION-TOF TOF.SIMS IV) confirmed the homogeneity of the coating composition through layer thickness (not shown). The (TiVCrZrHf)N coating demonstrated superior mechanical properties and high thermal stability. The extremely high hardness value of 48 GPa [8] confirmed that it has great potential for hard and protective coatings. The excellent thermal stability at 800 °C without silicide formation showed that the (TiVCrZrHf)N coating is a promising diffusion barrier material for Cu interconnection [11]. However, the special structural evolution of the (TiVCrZrHf)N coating has not been investigated yet in detail. According to previous reports, the special structural evolution become more significant when (TiVCrZrHf)N coating was deposited at high substrate temperature and high substrate bias voltage. Thus, this manuscript is dedicated to the microstructural evolution of a film deposited at high temperature and high bias voltage as a function of its thickness.

2. Experimental

The (TiVCrZrHf)N coatings were deposited on p-Si(100) wafers by a reactive radio-frequency magnetron sputtering system using

* Corresponding author at: Department of Materials Science and Engineering, National Chung Hsing University, Taichung 40227, Taiwan. Tel.: +886 4 2284 0500; fax: +886 4 2285 7017.
E-mail address: fsshieu@dragon.nchu.edu.tw (F.-S. Shieu).

0257-8972/$ – see front matter © 2012 Elsevier B.V. All rights reserved.
http://dx.doi.org/10.1016/j.surfcoat.2012.11.077

equimolar TiVCrZrHf targets that were 75 mm in diameter. Prior to deposition, Si substrates were cleaned and rinsed with ethanol and distilled water in an ultrasonic bath. The sputtering chamber was pumped down to 2.67×10^{-4} Pa using a turbo pump. (TiVCrZrHf)N coatings were deposited at a plasma power of 350 W in an $Ar+N_2$ mixed atmosphere under a working pressure of 6.67×10^{-1} Pa Flow rates of Ar and N_2 were maintained at 100 and 4 sccm, respectively. The distance between the substrate and target was 90 mm. Morphology was examined using field emission scanning electron microscopy (SEM, JEOL JSM-6700F). Microstructure and local composition were investigated by field emission transmission electron microscopy (TEM, FEI E.O. TecnaiF20) equipped with energy-dispersive spectroscopy (EDS) at an acceleration voltage of 200 kV. The chemical composition was determined by field-emission electron probe micro-analyses (FE-EPMA, JEOL JXA-8800M). The residual stress was determined by using the laser technology via measuring the substrate curvature and applying Stoney's equation for calculation. The nanohardness of the coatings was measured using a TriboLab nanoindenter (Hysitron).

3. Results and discussion

Fig. 1 shows the SEM micrographs of the as-grown (TiVCrZrHf)N coating deposited with different substrate temperatures and biases. Their deposition time was set at 60 min. Coatings without substrate bias revealed a typical V-shaped columnar structure with a faceted surface feature. When a bias was applied, the coating appears less defined but has a more densified columnar structure. These phenomena have been observed and explained in detail by our previous reports [8,9]. Interestingly, a very thick and featureless interlayer near the substrate was found when substrate bias and heat were applied. The thickness of the amorphous layer increased with the addition of the substrate bias voltage and substrate temperature. In order to analyze structure formation and its evolution, subsequent TEM characterizations were performed for a more detailed evaluation of microstructures. The nanohardness of the (TiVCrZrHf)N deposited at various processing parameters is listed in Table 1. The coating without a substrate bias and heating have a relative low hardness. As substrate bias and temperature increased, the hardness also increased. This is reasonable, because the coatings were more densified with the application of substrate biases and temperature [8,9]. The maximum hardness of 33.5 GPa was achieved when coating was deposited under substrate bias of −100 V and at substrate temperatures of 723 K. This demonstrates a moderate substrate bias and temperature to be necessary to obtain a good hard coating.

Cross-sectional TEM micrographs of as-grown (TiVCrZrHf)N coating deposited under substrate bias of −100 V and at substrate temperatures of 723 K are shown in Fig. 2. To fulfill the requirements of hard coating application, the (TiVCrZrHf)N coating was deposited at approximately 1.4 μm. There was a continuous change in structure of the (TiVCrZrHf)N coating through its whole thickness. Image contrast revealed that the coating had two distinct layers separated by a boundary (Fig. 2a). The four selected area diffraction (SAD) patterns were labeled as Zones A, B, C, and D. Zone A shows a mixed pattern of spots formed in Si wafer and halo ring. Zone B also has a halo ring. These findings confirm that that the structure near the substrate is amorphous. Noticeably, there are two extra spots around the (000) diffraction spot in Zone B, indicating a periodoc arrangement. Zone C contains arc-like FCC rings and a (200)-axis structure perpendicular to the substrate misaligned at ~50°. With increased coating thickness, this preferred orientation perpendicular to the substrate was transformed from (200) to (220). This angle of misalignment initially decreased and then became constant as coating thickness was further increased. Zone D contains a larger single grain SAD with (220)-axis FCC structure (Fig. 2c–f). These results are consistent with the observation of TEM dark-field image (Fig. 2b).

The HRTEM images of as-grown (TiVCrZrHf)N coating deposited under substrate bias of −100 V and at substrate temperatures of 723 K are presented in Fig. 3. An amorphous native oxide layer existed on the surface of the Si substrate. The (TiVCrZrHf)N layer grows on the substrate with a thick amorphous interfacial layer (Fig. 3a and b). Coincident with the SAD analysis in Fig. 2d, there is a layering amorphous structure with layer thickness of 2.29 nm between the amorphous and columnar regions (Fig. 3b inset). EDS analysis did not reveal any visible composition segregation, which may be due to the limited resolution. A more detailed investigation of the layering amorphous structure is still necessary. Fig. 3c and d shows HRTEM images near the bottom and upper part of the V-shaped column, respectively. Nanometer [200] out-of-plane oriented columns can be observed above the

Table 1
The stress and hardness of the (TiVCrZrHf)N deposited at various processing parameters.

Process parameter	Stress (GPa)	Hardness (GPa)
0 V, 723 K	0.62	10.0 ± 3.0
−50 V, 723 K	−2.14	22.5 ± 2.7
−100 V, 723 K	−5.11	33.5 ± 0.6
−150 V, 723 K	−5.32	32.6 ± 0.6
−200 V, 723 K	−5.94	32.4 ± 1.1
−100 V, RT	−5.62	24.5 ± 1.6
−100 V, 623 K	−5.35	32.9 ± 0.8
−100 V, 823 K	−5.01	32.5 ± 0.4

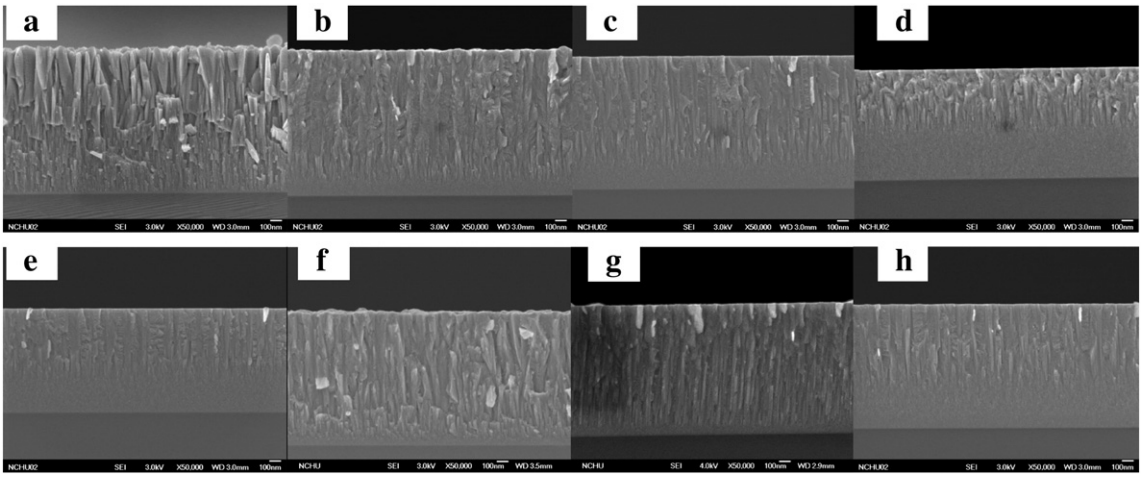

Fig. 1. The SEM micrographs of the as-grown (TiVCrZrHf)N coating deposited under different bias and at different substrate temperatures (a) 0 V, 723 K; (b) −50 V, 723 K; (c) −100 V, 723 K; (d) −150 V, 723 K; (e) −200 V, 450 °C; (f) −100 V, RT; (g) −100 V, 623 K; (h) −100 V, 823 K.

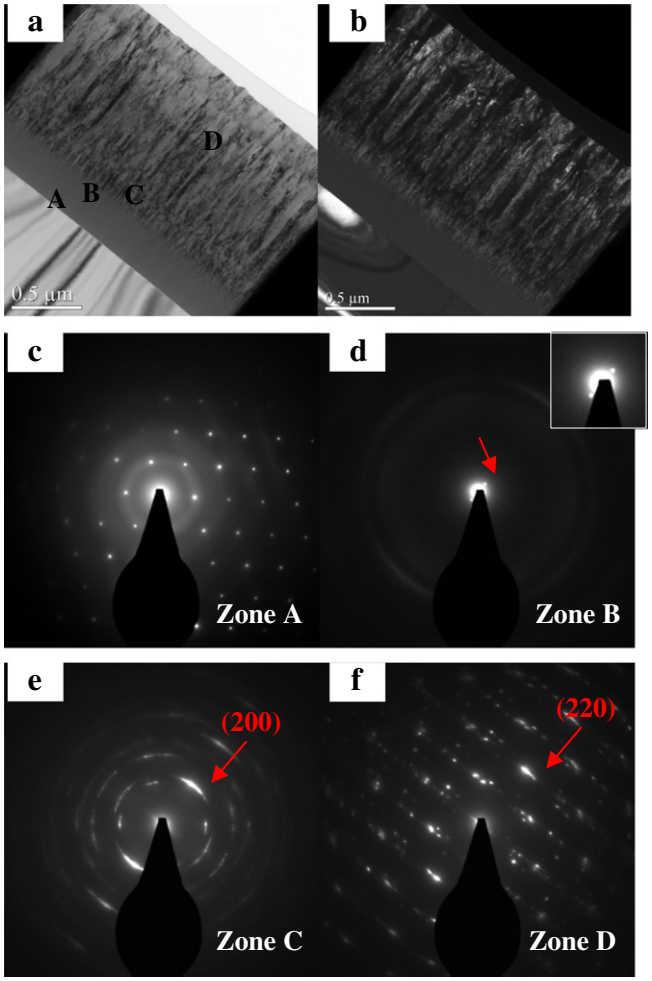

Fig. 2. Cross-sectional TEM micrographs of the as-deposited (TiVCrZrHf)N coatings deposited under substrate bias of −100 V and at substrate temperatures of 723 K. (a) Bright-field image. (b) Dark-field image. (c) SAD pattern of Zone A. (d) SAD pattern of Zone B. (e) SAD pattern of Zone C. (f) SAD pattern of Zone D.

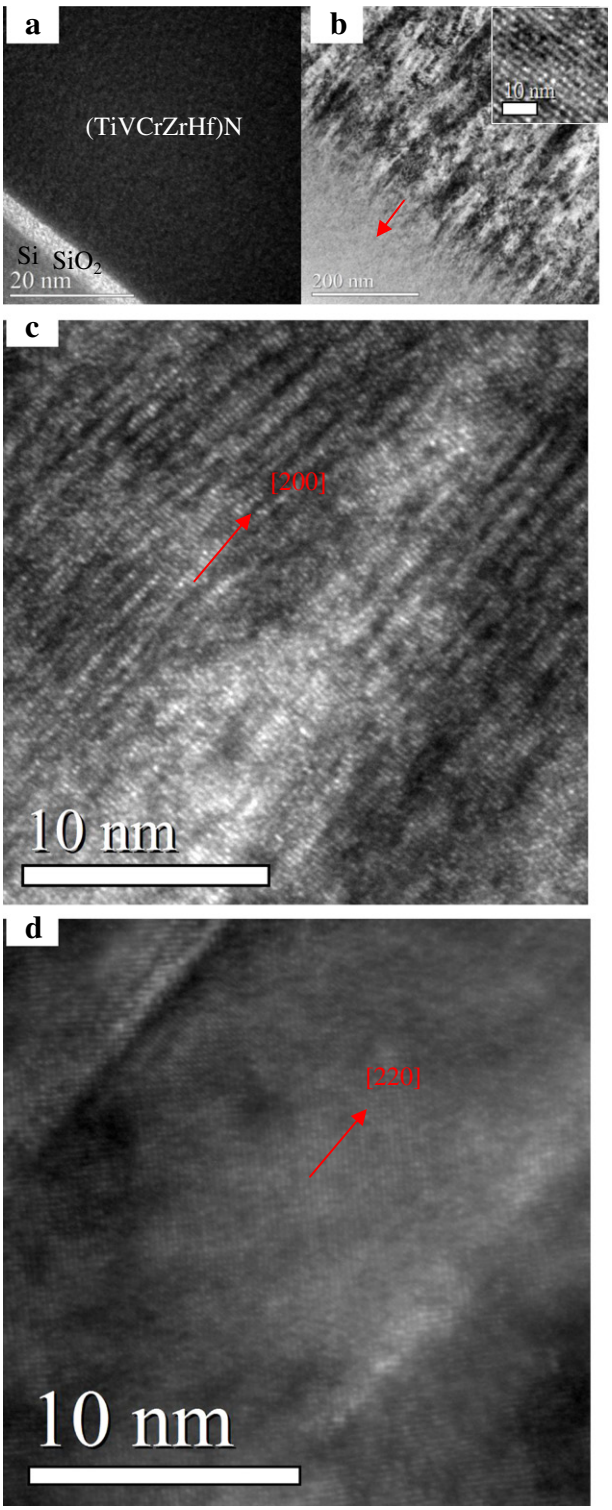

Fig. 3. HRTEM images of the as-deposited (TiVCrZrHf)N coatings deposited under substrate bias of −100 V and at substrate temperatures of 723 K. (a) Zone A of Fig. 2. (b) The interface of Zones B and C in Fig. 2. The inset is the image of layering amorphous structure, as indicated by the arrow. (c) Zone C of Fig. 2. (d) Zone D of Fig. 2.

amorphous layer. The interlayer spacing is about 0.216 nm, concurrent with that of FCC (200). However, the out-of-plane preferred orientation evolved from (200) to (220) as coating thickness was increased. The interplanar distance is approximately 0.154 nm, which is equal to that of FCC (220). In the case of a TiN coating, Li et al. [12,13] observed that the film was amorphous at a very early stage of film deposition (~1 nm), then randomly crystallized (2–6 nm), and finally formed the preferred orientation. As coating thickness increased, the preferred orientation changed from (200) to (111). The evolution of the preferred orientation has been discussed on the basis of surface energy and strain energy of the coating [14]. However, in this study, the preferred orientation was influenced by ion bombardment at a relatively high energy range. Previous studies have shown that for an NaCl crystal, a (220) or (200) orientation is expected because of ion channeling and lower energy loss in this more open direction over a long distance [15–18]. Since the (111) plane of the NaCl structure is more densely packed than other planes, the (111) plane has higher resputtering probabilities. Accordingly, the (200) orientation was expected at small thickness and the (220) orientation was favored at large thickness in this study.

The growth of the (TiVCrZrHf)N coating can be concluded and summarized according to TEM findings. Interestingly, we observed that a 270-nm thick amorphous (TiVCrZrHf)N layer begins near the substrate and then a transition from amorphous to crystal structure occurs. The main reason for variations in film microstructure is still unclear. In general, the several nm-thick interfacial amorphous layer can be attributed to the initial nitride or oxidation process and the large lattice mismatch between coating and substrate [19–21]. However, in most previous studies, the interfacial amorphous layer still formed even after the native oxide layer of the Si substrate was removed [20,21]. Moreover, we did not observe epitaxy growth in the present study. The lattice mismatch and interdiffusion between

coating and substrate may induce strain and result in local lattice distortion only. It is insufficient and cannot fully explain the formation of the thick amorphous layer. In addition to the substrate effect, we propose several factors that may contribute to the mechanism behind the growth of (TiVCrZrHf)N on Si wafer. (i) According to our previous report [9], the resputtering effect and thus the renucleation rate can be significantly enhanced with increased substrate bias voltage. This hindered the formation of the crystal structure, leading to an increase in the thickness of the amorphous interfacial layer. (ii) In some cases, crystallinity may decrease with an increase in substrate temperature. Crystallinity is reduced at high temperatures, probably due to the instability and adatom desorption at these temperatures [1,22,23]. The EPMA element contents in as-grown (TiVCrZrHf)N coating deposited with different substrate temperatures and biases are shown in Fig. 4. The metal content is seen to be almost independent of the substrate bias. However, the content of N is found to decrease significantly with increasing applied substrate temperature. This suggests that the higher obtained energy at higher substrate temperature can let some N atoms in disequilibrium sites escape from the surface. Accordingly, the decreased N triggered the decrease of crystallite size, leading to the amorphization of the coating structure. Results of the present study provide direct experimental evidence that the amorphous interlayer can be thickened when deposition is performed at higher substrate bias and temperature (Fig. 1) [8,9]. (iii) The coating fabricated at higher substrate bias contains higher intrinsic compressive stress (~6.3 GPa). This stress is considered to originate from the well-known atomic-peening effect, whereby the impinging ions knock surface atoms deeper into the film, where they become trapped. Intrinsic compressive stress may also promote the amorphization of the coating structure. Thermal stress, which results from the differences in the coefficient of thermal expansion (CTE) between the coating and substrate, can be ignored in this study [2]. The CTE of the coating, estimated from the rule of mixtures, is $6.4\times10^{-6}\ K^{-1}$. Since the CTE of the coating is larger than that of the Si substrate, the thermal stress was calculated to be tensile at about 0.5 GPa. As seen in Fig. 1 and Table 1, a thick amorphous interlayer was formed when the intrinsic compressive stress in coatings is high. Hu and Song et al. have proposed that the formation of amorphous layer is a way for stress relaxation [24,25]. Therefore, the large stress may be contributive to induce the formation of amorphous layer. (iv) As previously mentioned, multi-principal component nitride coatings have highly distorted lattices and thus inhibit crystal growth due to the variation among atomic sizes of the target elements. The combination of these four factors induced the formation of a thick amorphous interlayer in this study. Based on previous reports, the determination of the multi-principal components is an important issue for the expansion of the amorphous interlayer.

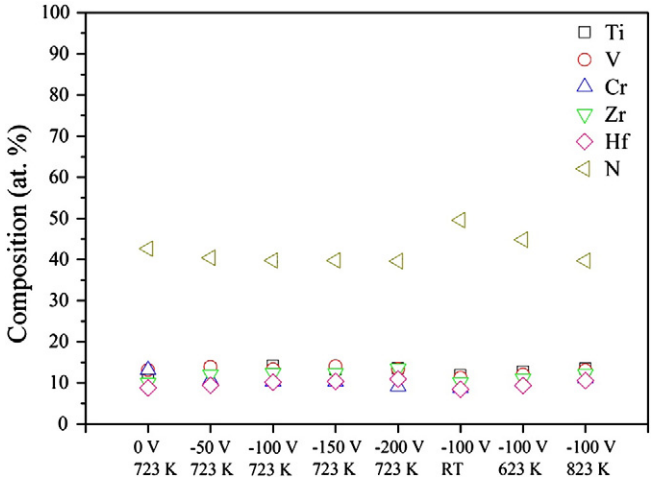

Fig. 4. EPMA element contents in (TiVCrZrHf)N coatings deposited under different bias and at different substrate temperatures.

4. Conclusion

In summary, we have successfully deposited (TiVCrZrHf)N coating on Si substrate by conventional sputtering method. Microstructure analysis revealed that the coatings are characterized by a continuous variation in structure from amorphous to columnar with FCC phase. The amorphous interlayer was observed to be about 270 nm. Under the appropriate process parameters, the resultant coatings were unlike the nitrides reported in previous studies (binary nitride in particular), which had a nanometer-thick amorphous interlayer near the substrate only. The incorporation of different-sized elements may be greatly beneficial for the formation of an amorphous interlayer. In addition, out-of-plane preferred orientation evolved from (200) to (220) as coating thickness increased, probably due to the resputtering effect caused by energetic ion bombardment. Accordingly, (TiVCrZrHf)N needs a substrate bias of −100 V and substrate temperature of 723 K to form dense and mechanically stable coating. The maximum hardness of around 33.5 GPa is obtained.

Acknowledgment

The authors gratefully acknowledge the financial support for this research by the National Science Council of Taiwan under grant no. NSC100-2221-E-005-034-MY3.

References

[1] C.H. Lai, M.H. Tsai, S.J. Lin, J.W. Yeh, Surf. Coat. Technol. 201 (2007) 6993.
[2] P.K. Huang, J.W. Yeh, Thin Solid Films 518 (2009) 180.
[3] M.H. Tsai, C.H. Lai, J.W. Yeh, J.Y. Gan, J. Phys. D: Appl. Phys. 41 (2008), (235402-1-7).
[4] J.W. Yeh, S.K. Chen, S.J. Lin, J.Y. Gan, T.S. Chin, T.T. Shun, C.H. Tsau, S.Y. Chang, Adv. Eng. Mater. 6 (2004) 299.
[5] P.K. Huang, J.W. Yeh, T.T. Shun, S.K. Chen, Adv. Eng. Mater. 6 (2004) 74.
[6] Y.J. Zhou, Y. Zhang, Y.L. Wang, G.L. Chen, Appl. Phys. Lett. 90 (2007), (181904-1-3).
[7] V. Braic, M. Balaceanu, M. Braic, A. Vladescu, S. Panseri, A. Russo, J. Mech. Behav. Biomed. Mater. 10 (2012) 197.
[8] S.C. Liang, Z.C. Chang, D.C. Tsai, Y.C. Lin, H.S. Sung, M.J. Deng, F.S. Shieu, Appl. Surf. Sci. 257 (2011) 7709.
[9] D.C. Tsai, S.C. Liang, Z.C. Chang, Z.C. Chang, T.N. Lin, M.H. Shiao, F.S. Shieu, Surf. Coat. Technol. 207 (2012) 293.
[10] S.C. Liang, D.C. Tsai, Z.C. Chang, H.S. Sung, Y.C. Lin, Y.J. Yeh, M.J. Deng, F.S. Shieu, Appl. Surf. Sci. 258 (2011) 399.
[11] S.C. Liang, D.C. Tsai, Z.C. Chang, Z.C. Chang, T.N. Lin, M.H. Shiao, F.S. Shieu, Electrochem. Solid State Lett. 15 (2012) H5.
[12] T.Q. Li, S. Noda, H. Komiyama, T. Yamamoto, Y. Ikuhara, J. Vac. Sci. Technol. A 21 (2003) 1717.
[13] T.Q. Li, S. Noda, Y. Tsuji, T. Ohsawa, H. Komiyama, J. Vac. Sci. Technol. A 20 (2002) 583.
[14] J. Pelleg, L.Z. Zevin, S. Lungo, N. Croitoru, Thin Solid Films 197 (1991) 117.
[15] N.H. Hoang, D.R. McKenzie, W.D. McFall, Y. Yin, J. Appl. Phys. 80 (1996) 6279.
[16] M.K. Lee, H.S. Kang, W.W. Kim, J.S. Kim, W.J. Lee, J. Mater. Res. 12 (1997) 2393.
[17] J.-C. Lin, G. Chen, C. Lee, J. Electrochem. Soc. 146 (1999) 1835.
[18] J.-C. Lin, C. Lee, J. Electrochem. Soc. 147 (2000) 713.
[19] K.S. Stevens, M. Kinniburgh, A.F. Schwartzman, A. Ohtani, R. Beresford, Appl. Phys. Lett. 66 (1995) 3179.
[20] J.H. Choi, J.Y. Lee, J.H. Kim, Thin Solid Films 384 (2001) 166.
[21] J.X. Zhang, Y.Z. Chen, H. Cheng, A. Uddin, Shu Yuan, K. Pita, T.G. Andersson, Thin Solid Films 471 (2005) 336.
[22] H. Jiménez, E. Restrepo, A. Devia, Surf. Coat. Technol. 201 (2006) 1594.
[23] B. Subramanian, K. Ashok, P. Kuppusami, C. Sanjeeviraja, M. Jayachandran, Cryst. Res. Technol. 43 (2008) 1078.
[24] G. Hu, X. Kong, Y. Wang, L. Wan, X. Duan, J. Mater. Sci. Lett. 22 (2003) 1581.
[25] J.H. Song, S.C. Wang, J.C. Sung, J.L. huang, D.F. Lii, Thin Solid Films 517 (2009) 4753.